Grafting of Molecularly Imprinted Polymers from the Surface of Fe₃O₄ Nanoparticles Containing Double Bond via Suspension Polymerization in Aqueous Environment: A Selective Sorbent for Theophylline

Xubiao Luo, Fang Deng, Shenglian Luo, Xinman Tu, Lixia Yang

School of Environmental and Chemical Engineering, Nanchang Hangkong University, Nanchang 330063, People's Republic of China

ABSTRACT: Molecularly imprinted polymers (MIPs) were grafted from the surface of Fe₃O₄ nanoparticles containing double bond via suspension polymerization in aqueous environment, and the leakage of Fe₃O₄ nanoparticles from MIPs was overcome in this study. The effect of different cross-linker on adsorption capacity of the resultant magnetic MIPs was investigated using pure trimethylolpropane trimethacrylate (TRIM) or the mixture of TRIM and divinylbenzene (DVB) as cross-linker. Both magnetic MIPs exhibited higher adsorption capacity for the template theophylline than the corresponding non-imprinted polymer, and Freundlich model fitted reasonably well for theophylline adsorption on both magnetic MIPs. In addition, both magnetic MIPs exhibited good recognition properties for the template theophylline versus caffeine, and the selectivity of magnetic MIPs using pure TRIM as cross-linker (mag-MIP-TRIM) was much higher than those using the mixture of TRIM and DVB as cross-linker (mag-MIP-TRIM and DVB). The adsorption dynamics of theophylline on both magnetic MIPs fitted well with the first-order kinetic model, but the adsorption equilibrium on mag-MIP-TRIM and DVB reached faster than that on mag-MIP-TRIM. © 2011 Wiley Periodicals, Inc. J Appl Polym Sci 121: 1930–1937, 2011

Key words: magnetic molecularly imprinted polymer; suspension polymerization; adsorption dynamics; theophylline

INTRODUCTION

Molecularly imprinted polymers (MIPs) are stable synthetic polymers possessing specific molecular recognition sites. With the advantages of MIPs, such as mechanical/chemical stability, low cost, and reusability, MIPs have wide application in many fields.[1–6] However, the various application of MIPs are limited by the tedious separation process. Recently, a technique based on magnetic separation has received increasing attention.[7] When magnetically susceptible materials can be encapsulated in MIPs, magnetic MIPs will not only have magnetically susceptible characteristic but also have selectivity for the guest molecule.[8]

By far, many methods have been developed to prepare magnetic MIPs, such as alumina template,[9] miniemulsion polymerization,[10,11] core-shell emulsion polymerization,[12] "semi-covalent" imprinting technique,[13] and suspension polymerization.[14–20] Suspension polymerization has been a most popular method for the preparation of porous magnetic MIPs with spherical or particle shape. By encapsulating magnetic iron oxide, the superparamagnetic composite MIPs were prepared by suspension polymerization in perfluorocarbon liquid for the first time.[14] In some reports, Fe₃O₄ nanoparticles modified with oil acid or poly(ethylene glycol) were used to prepare magnetic MIPs.[15–20] However, the bonding force between Fe₃O₄ and MIPs is weak, Fe₃O₄ nanoparticles can not be encapsulated by MIPs efficiently and might leak from MIPs, leading to the reduction of magnetic response.

The leakage of Fe₃O₄ from MIPs can be overcome by grafting techniques. Grafting polymerization on inorganic nanoparticles could be carried out either by the "grafting from" or "grafting to" methods.[21,22] The "grafting from" technique can produce a high grafting density on the surface of solid support because of the highly selective occurrence of polymerization. However, the most disadvantage of "grafting to" method is time-consuming and poorly

reproducible, and the grafting density is low. Recently, the "grafting from" technique has been used by several research groups to produce imprinted polymer films on various substrates.[23–27]

There is only one report that the surface functionalized Fe_3O_4 nanoparticles with double bonds were used to prepare magnetic MIPs in silicone oil.[28] MIPs prepared in low polar organic solvents demonstrate their best performance in hydrophobic organic solvent such as chloroform or acetonitrile.[29] However, these MIPs display poor recognition of the target compound in aqueous environment, which limit various application of MIPs.[4,30] Therefore, the MIPs prepared in aqueous environment are desired for effective molecular recognition of target analytes in water phase.[4] There have been some approaches and strategies to prepare magnetic imprinted polymers in aqueous environment such as atom transfer radical polymerization.[31] However, till now, no work has been reported about the magnetic MIPs which were prepared by "grafting from" technique by applying Fe_3O_4 nanoparticles containing double bonds as magnetically susceptible material via suspension polymerization in aqueous environment.

In the present work, the Fe_3O_4 nanoparticles were surface-modified with 3-(trimethoxysilyl)propyl methacrylate (TMSMA) which introduced the double bonds onto the surface of Fe_3O_4 nanoparticles to form grafting sites. The magnetic MIPs were prepared by "grafting from" method via suspension polymerization using surface-modified Fe_3O_4 as magnetically susceptible material in aqueous environment. Then, the characteristics and molecular recognition property of the magnetic MIPs in aqueous environment were investigated.

EXPERIMENTAL

Materials

Trimethylolpropane trimethacrylate (TRIM) was obtained from Jiangsu Tianpeng Tongren Fine Chemical Co. (Jiangsu, China). Ferric chloride ($FeCl_3 \cdot 6H_2O$), methacrylic acid, methanol, and ethanol were purchased from Shantou Xilong Chemical Co. (Shantou, China). Ferrous sulfate ($FeSO_4 \cdot 7H_2O$) was obtained from Tianjin Fuchen Reagent Plant (Tianjin, China). Divinylbenzene (DVB), theophylline, and caffeine were supplied by Pure Crystal Shanghai Reagent Co. (Shanghai, China). Toluene, azo(bis)-isobutyronitrile and poly(ethylene glycol) 6000 (PEG6000) were purchased from Shanghai Qingxi Chemical Plant (Shanghai, China). Ammonium hydroxide was purchased from Jiangxi Hongdou Biochemical Co. (Nanchang, China). 3-(Trimethoxysilyl)-propyl methacrylate (98%) was purchased from Sigma-Aldrich (St. Louis, MO). Water was purified

through a Milli-Q water system (Bedford, MA). All other reagents were of analytical grade.

Preparation of Fe_3O_4 magnetic nanoparticles

The Fe_3O_4 magnetic nanoparticles were prepared according to Ref.[28] with minor modification. $FeCl_3 \cdot 6H_2O$ (24.3 g) and $FeSO_4 \cdot 7H_2O$ (16.7 g) were dissolved in 200 mL distilled water and heated to 90°C. Ammonium hydroxide (60 mL) was rapidly added. After 3 h, the sediment was washed with distilled water until neutral.

Modification of Fe_3O_4 nanoparticles with TMSMA

The pH of 100 mL 95% ethanol solution was adjusted by acetic acid. When pH is between 4 and 5, 10 mL TMSMA was added. TMSMA was hydrolyzed 5 min under ultrasound. The magnetic Fe_3O_4 nanoparticles were added into the above solution, and the mixture was stirred for 24 h at 50°C. The magnetic nanoparticles modified with TMSMA were washed with ethanol and then were dispersed in ethanol to form a ferrofluid.

Grafting of molecularly imprinted polymer from Fe_3O_4

The magnetic MIPs were prepared as follows:

a. The theophylline (1.0 mmol) and MAA (4.0 mmol) was dissolved in 30 mL methanol. This mixture was stored in dark for 12 h for preparation of preassembly solution.
b. AIBN (0.1 g) was dissolved in 4 mL toluene.
c. The PEG6000 (8.0 g) was dissolved in 75 mL water in a three-necked flask, and then 10 mL of the ethanol ferrofluid was added. The mixture was under ultrasound for 30 min.
d. The cross-linker (20 mmol pure TRIM or the mixture of 10.0 mmol TRIM and 10.0 mmol DVB) was mixed with the preassembly solution prepared by step (a). This mixture was added into the three-necked flask, and then AIBN solution was added into it.
e. The above mixture was stirred at 300 rpm and purged with nitrogen gas to displace oxygen, and then the three-necked flask was placed in water-bath in which the temperature was 70°C. The reaction was allowed to proceed at 70°C for 8 h.
f. After the polymerization, the magnetic MIPs were collected by an external magnetic field, and washed with methanol : acetic acid solution (9 : 1, v/v) in a soxhlet extraction system until the template could not be detected by HPLC. The polymers were washed with water three times again and dried at 60°C.

The magnetic non-imprinted polymers (NIPs) were prepared and processed similarly as above, except that the template molecule theophylline was not added.

Steady-state binding studies

Hundred milligrams of magnetic MIPs were placed in a 100-mL conical flask and mixed with 20 mL theophylline solution with specific initial concentrations ranging from 0.5 to 5.0 mmol L^{-1}. The samples were oscillated in a thermostatic oscillator (Changzhou Guohua Instrument Company, Changzhou, China) at $25°C$ for 24 h. The magnetic MIPs were separated under an external magnetic field. The concentration of free theophylline in the solution was measured by HPLC at 272 nm. In addition, the amount of theophylline adsorbed to the magnetic NIPs was also determined in parallel. The adsorption capacity (q) was calculated as follows:

$$q = (C_0 - C_t)V/W \qquad (1)$$

where C_0 (mmol/L) is the initial theophylline concentration, C_t (mmol/L) is the theophylline concentration of difierent time, V (mL) is the volume of theophylline solution, and W (g) is the mass of the magnetic MIPs.

The imprinting eficiency (IE) of the magnetic MIPs was defined as follows:

$$IE = q_{MIP}/q_{NIP} \qquad (2)$$

where q_{MIP} and q_{NIP} are the q_e of the magnetic imprinted and corresponding non-imprinted microspheres, and q_e is the amount of theophylline bound to MIPs or NIPs at equilibrium.

Competitive batch rebinding tests

In the competitive batch rebinding tests, the selectivity of the imprinted particles was studied in a binary theophylline-caffeine solution. The magnetic MIPs were subjected to a binary mixture of theophylline and caffeine with individual initial concentrations of 0.1 mmol/L. The adsorption mixture were oscillated in a thermostatic oscillator for 24 h and analyzed similarly as in steady-state binding studies above. The following equations were used to quantify the selectivity of the magnetic MIPs. The recognition selectivity was evaluated by the static distribution coefficient (K_D) and seperation factor (α). K_D and α were defined as follows:

$$K_D = C_p/C_s \qquad (3)$$

where C_p is the amount of ligand adsorbed and C_s is the free ligand concentration.

$$\alpha = K_{D1}/K_{D2} \qquad (4)$$

where K_{D1} and K_{D2} are the static distribution coefficients of template and control molecules.

Adsorption dynamics of the magnetic MIPs

Hundred milligrams of magnetic MIPs were placed in a 100-mL conical flask and mixed with 20 mL 4.0 mmol/L theophylline solution. The conical flask was oscillated in a thermostatic oscillator with constant temperature at $25°C$ for difierent time intervals. The concentration of theophylline in the solution was determined by HPLC at 272 nm. The adsorption capacity was calculated according to eq. (1).

Characterization

Fourier transform infrared (FTIR) spectra was recorded on a Varian scimitar 2000 (Varian Corp. Las Vegas, USA).

Magnetic characteristics of Fe_3O_4 and magnetic MIPs were measured by using LDJ-9600 vibrating sample magnetometer (VSM, America LDJ Company).

RESULTS AND DISCUSSION

Synthesis of magnetic MIPs by "grafting from" technique via suspension polymerization

The synthesis of the magnetic MIPs through a multistep procedure is illustrated in Figure 1. First, superparamagnetic Fe_3O_4 nanoparticles were prepared by the coprecipitation method. Then, the Fe_3O_4 nanoparticles were surface-modified with TMSMA which introduced double bonds onto the surface of Fe_3O_4 nanoparticles to form grafting sites. During the synthesis procedure of the magnetic MIPs, the magnetic Fe_3O_4 nanoparticles can be fixed in the MIPs because of the double bonds, which were covalently bonded to the Fe_3O_4 nanoparticles, and can react with crosslinker and MAA. Consequently, the leakage of Fe_3O_4 nanoparticles from the MIPs can be effectively prevented. Finally, the magnetic MIPs were washed with methanol/acetic acid solution in a soxhlet extraction system to remove the template molecules and leave recognition sites there. Our investigation shows that the magnetic response, adsorption capacity, and selectivity of the obtained magnetic MIPs are hardly reduced even in the fifth cycle of reuse.

Control experiment was performed by applying the Fe_3O_4 without TMSMA modification as magnetically susceptible material to illustrate the function of the double bonds. After polymerization, it was found that some Fe_3O_4 nanoparticles were set apart from MIPs, and the others were encapsulated in MIPs. MIPs without magnetic response and magnetic MIPs with poor magnetic response were obtained. The leakage of
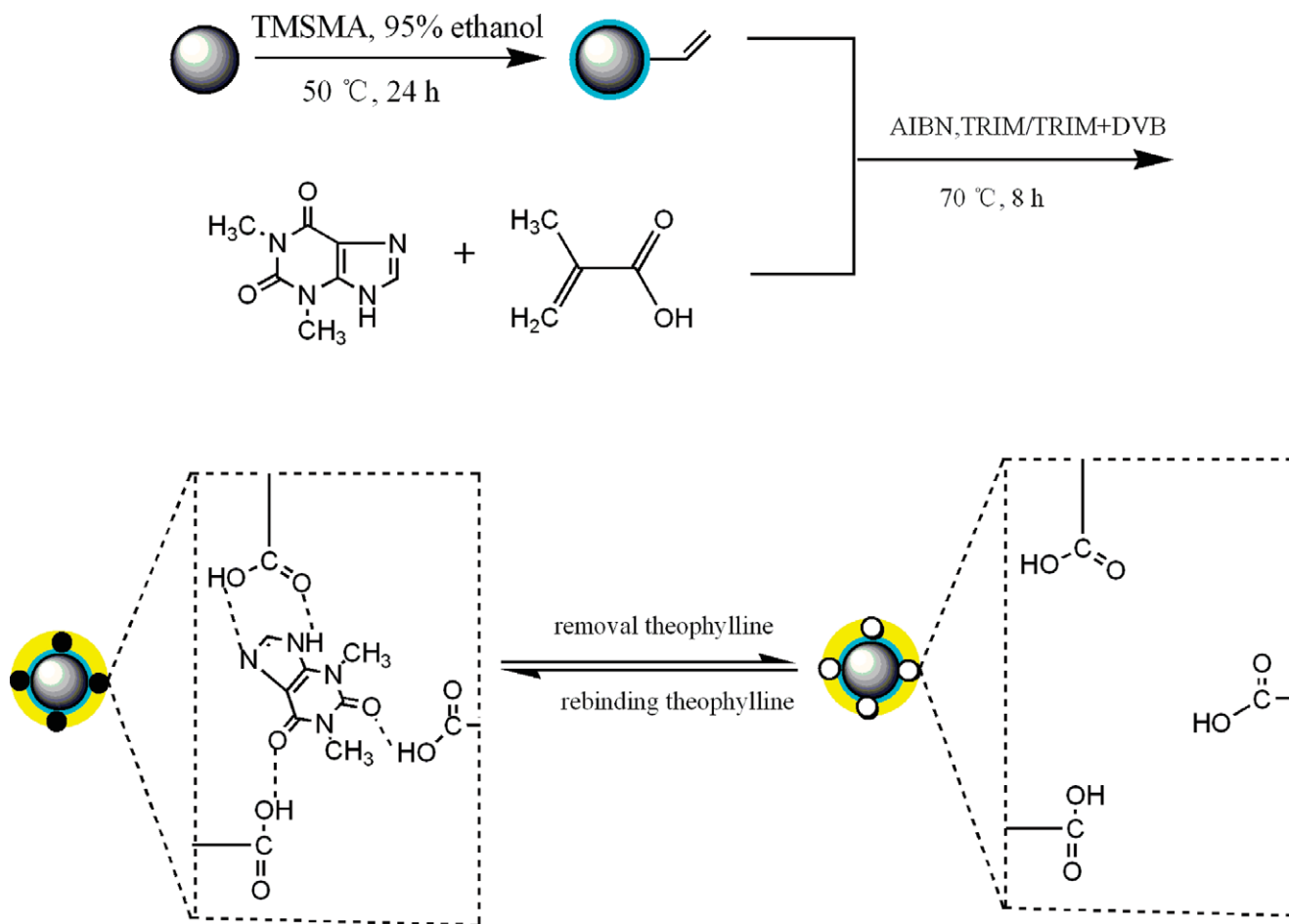
Figure 1 Schematic representation of grafting of molecularly imprinted polymers from the surface of Fe_3O_4 nanoparticles. [Color figure can be viewed in the online issue, which is available at wileyonlinelibrary.com.]

the Fe_3O_4 nanoparticles from the MIPs resulted in the poor magnetic response, which was caused by the weak bonding force because of the lack of the double bonds on the surface of Fe_3O_4 nanoparticles. Consequently, the "grafting from" procedure is necessary in the study.

FTIR analysis

Grafting of MIPs from the surface of Fe_3O_4 nanoparticles is confirmed by FTIR spectroscopy measurements. FTIR spectroscopy of Fe_3O_4 shows that the strong peaks at 3434 cm^{-1} represent the stretching vibration of O—H, the strong peaks at 590 cm^{-1} represent the stretching vibration of Fe—O [Fig. 2(a)], which indicate the presence of hydroxyl group on the surface of Fe_3O_4 nanoparticles. The FTIR spectroscopy of Fe_3O_4 shifts dramatically after the modification by TMSMA [Fig. 2(b)]. The new peaks at 1096 cm^{-1}, 1027 cm^{-1}, and 802 cm^{-1} represent the stretching vibration of Si—O. The weak peaks at 1652 cm^{-1} and 1699 cm^{-1} are attributed to the stretching vibration of C=C and C=O, respectively. The stretching vibration of Fe—O at 590 cm^{-1} is

observed. These peaks indicate that the surface of Fe_3O_4 nanoparticles is modified by TMSMA. After the preparation of magnetic MIPs, the stretching vibration of C=C at 1652 cm^{-1} disappears [Fig. 2(c,d)]. The peaks of C=O become strong and are shifted from 1699 cm^{-1} to 1720 cm^{-1}, suggesting that TMSMA is polymerized with MAA and cross-linker. In all samples, the peaks at 1636 cm^{-1} are attributed to plenty of water.
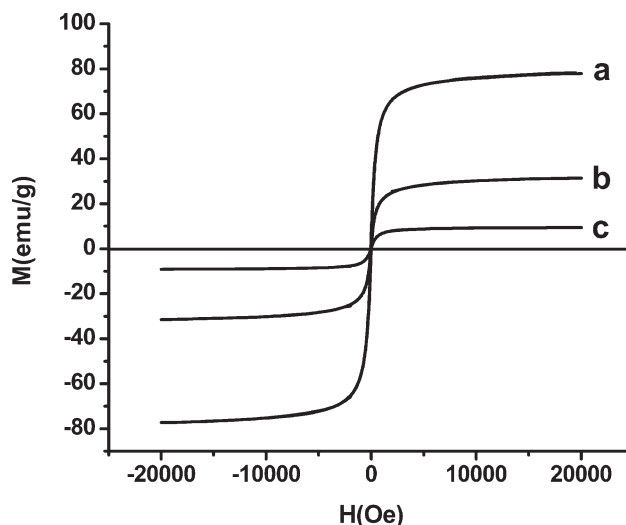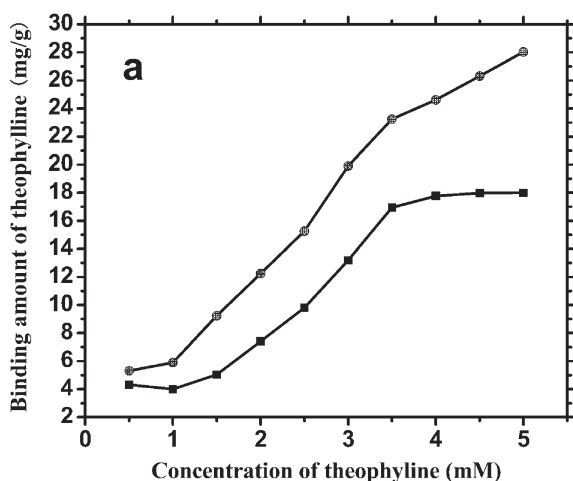
Magnetic characteristics of MIPs

Figure 3 shows the plots of magnetization versus magnetic field (M-H loop) at 25°C for the Fe_3O_4 and magnetic MIPs, respectively. It is apparent that there is no hysteresis, and both remanence and coercivity are zero, suggesting that the samples are superparamagnetic. Superparamagetism of these samples illustrates that Fe_3O_4 and both the magnetic MIPs respond magnetically to an external magnetic field and that this response vanishes upon the removal of the field. The saturation magnetization of Fe_3O_4 nanoparticles is 77.74 emu/g. After encapsulation by MIPs, the saturation magnetization of the resultant
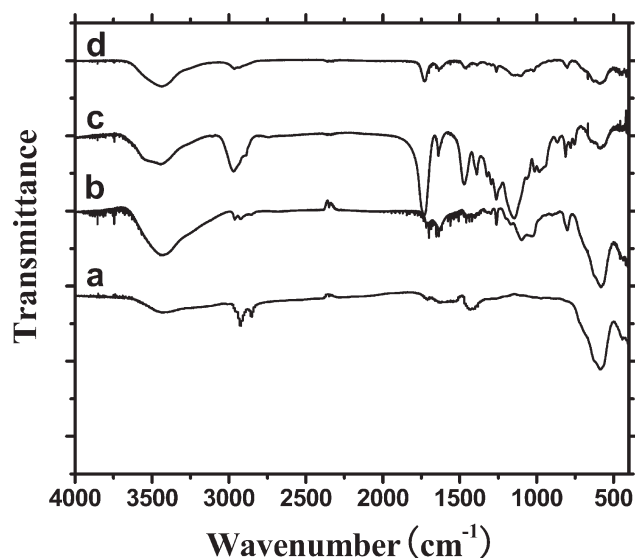
Figure 2 FTIR spectra of (a) Fe_3O_4, (b) Fe_3O_4 modified with TMSMA, (c) magnetic MIPs using pure TRIM as cross-linker (mag-MIP-TRIM), and (d) magnetic MIPs using the mixture of TRIM and DVB as cross-linker (mag-MIP-TRIM and DVB).

Figure 3 Magnetization curve at 298 K with (a) Fe_3O_4, (b) mag-MIP-TRIM and DVB, and (c) mag-MIP-TRIM.

magnetic MIPs drops significantly (9.249 emu/g for mag-MIP-TRIM and 31.43 emu/g for mag-MIP-TRIM and DVB). The decrease in magnetization value of magnetic MIPs indicates that the polymeric coating has a strong impact on the magnetism of the Fe_3O_4 and shields the magnetite effectively, thus significantly reducing their magnetic response toward the external magnetic field. However, the saturation magnetization value of these magnetic MIPs is high enough for magnetic separation with a conventional magnet, and the magnetic MIPs could be easily and quickly separated from a sample solution within a short time through placing a strong magnet in the separation step.

Molecular recognition property

The recognition ability of the magnetic MIPs toward the template theophylline was investigated by the steady-state binding method. As shown in Figure 4, both mag-MIP-TRIM and mag-MIP-TRIM and DVB exhibit higher capacity for theophylline than the corresponding magnetic NIPs. In addition, the adsorption capacity of magnetic NIPs using the mixture of TRIM and DVB as cross-linker (mag-NIP-TRIM and DVB) is much lower than that of magnetic NIPs using pure TRIM as cross-linker (mag-NIP-TRIM). The imprinting efficiency of mag-MIP-TRIM and DVB is larger than 5, but that of mag-MIP-TRIM is less than 2. The differences in the imprinting efficiency between mag-MIP-TRIM and mag-MIP-TRIM and DVB could be ascribable to that the number of nonspecific interaction sites of mag-MIP-TRIM is more than mag-MIP-TRIM and
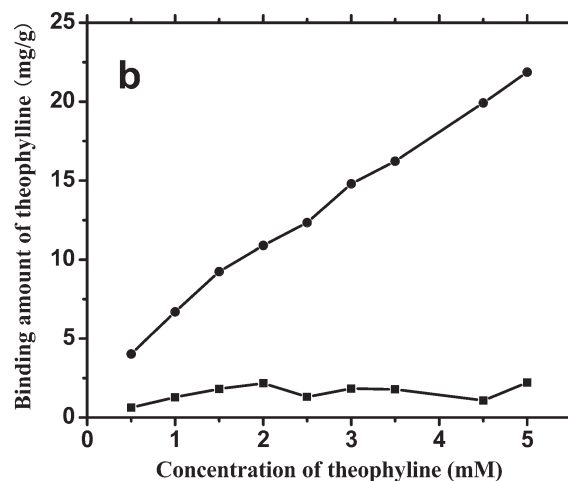
Figure 4 (a) Amount of theophylline bound by mag-MIP-TRIM (●) and mag-NIP-TRIM (■) and (b) Amount of theophylline bound by mag-MIP-TRIM and DVB (●) and mag-NIP-TRIM and DVB (■).
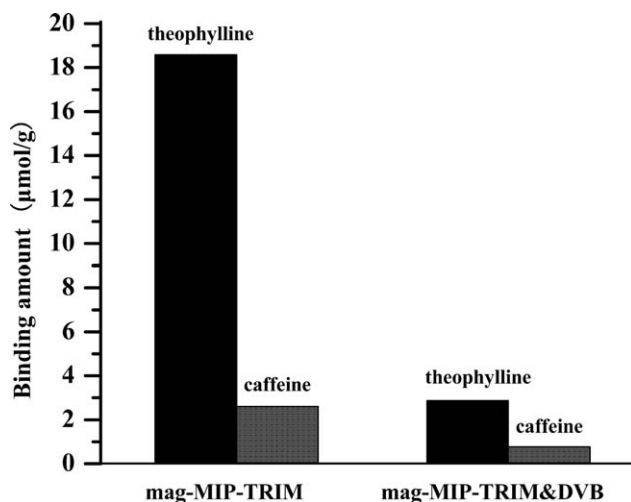
Figure 5 Binding behaviors of different compounds on the theophylline imprinted mag-MIP-TRIM and mag-MIP-TRIM and DVB. Experiment was conducted by the addition of 100 mg magnetic MIPs in 0.1 mM analyte solution (20 mL) at room temperature.

DVB. It is plausible that the C—O—C and C=O groups of TRIM could interact with N—H groups of the theophylline by hydrogen bond interaction, while there is no such sites for DVB.

The binding selectivity by mag-MIP-TRIM and mag-MIP-TRIM and DVB toward theophylline against its structural analog—the caffeine was compared. It can be seen from Figure 5 that both mag-MIP-TRIM and mag-MIP-TRIM and DVB show much higher adsorption to theophylline than caffeine, which indicates that both magnetic MIPs exhibit higher selectivity for imprinting molecule theophylline than caffeine. In addition, the seperation factors are 87.3 and 3.8 for mag-MIP-TRIM and mag-MIP-TRIM and DVB, respectively, indicating that the selectivity of mag-MIP-TRIM is much higher than mag-MIP-TRIM and DVB.

Compared with magnetic imprinted polymer nanowires,[9] although the molecular recognition property of the magnetic MIPs was carried out in aqueous environment in our study, the adsorption capacity and the selectivity of magnetic MIPs in our study are similar to, or even better than those of magnetic imprinted nanowires for theophylline recognition in acetonitrile.

Adsorption isotherm

The isotherm models of Langmuir and Freundlich were used to fit the experimental adsorption equilibrium data of theophylline on magnetic MIPs in the present study:

Langmuir equation

$$C_e/q_e = (1/K_{L \cdot q_m}) + (1/q_m)C_e \qquad (5)$$

where C_e (mg/L) is the concentration of theophylline at equilibrium, q_e is the mass of theophylline adsorbed per mass of magnetic MIPs at equilibrium, q_m (mg/g) is the maximum amount of theophylline adsorbed per unit mass of the magnetic MIPs corresponding to complete monolayer coverage, and K_L (L/mg) is the Langmuir constant. The Langmuir model assumes that the surface of the adsorbent is homogeneous, covered with only one type of adsorption site.

Freundlich equation

The Freundlich isotherm model is frequently used to account for heterogeneous binding sites in MIPs.[32,33]

$$q_e = K_F C_e^{1/n} \qquad (6)$$

where K_F and n are the Freundlich constants related to the adsorption capacity and intensity respectively,
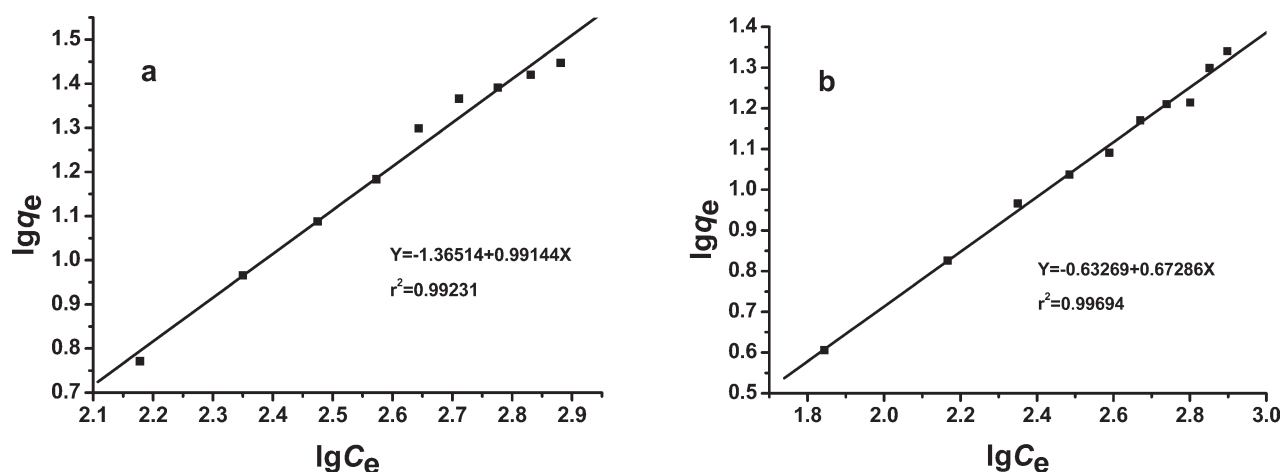
Figure 6 Relationship curves of lgq_e and lgC_e according to Freundlich equation: (a) mag-MIP-TRIM and (b) mag-MIP-TRIM and DVB.

TABLE I
Langmuir and Freundlich Isotherm Constants of Magnetic MIPs

Magnetic MIPs	Langmuir isotherm model			Freundlich isotherm model		
	q_m (mg/g)	K_L (L/mg)	r^2	K_F ($mg^{1-(1/n)}$ $L^{1/n}$ g^{-1})	n	r^2
mag-MIP-TRIM	94.43	5.61×10^{-4}	0.574	0.0421	1.0086	0.992
mag-MIP-TRIM and DVB	37.38	1.45×10^{-3}	0.946	0.2124	1.4866	0.997

and q_e is the mass of theophylline adsorbed per mass of magnetic MIPs at equilibrium. When n is higher than 1, the adsorption is favorable. When n is equal to 1, the adsorption is linear. When n is less than 1, the adsorption is unfavorable.

The correlation coeficients and other isotherm constants in the Langmuir and Freundlich equations, obtained by calculation from the slopes and intercepts of the plots (only the relationship curves of lgq_e and lgC_e according to Freundlich equation is given in Fig. 6), are summarized in Table I. The linear plot for Langmuir adsorption isotherm poorly describe the present isotherm adsorption data ($r^2 = 0.574$ and 0.946). Regression coefficients (r^2) of theophylline on both magnetic MIPs are larger than 0.99 in Freundlich equations, indicating that Freundlich model fits reasonably well for theophylline adsorption on both magnetic MIPs. The Freundlich adsorption intensity parameter (n value) is 1.0086 for mag-MIP-TRIM, which is close to 1, indicating the linear adsorption of theophylline on mag-MIP-TRIM. The Freundlich adsorption intensity parameter for mag-MIP-TRIM and DVB is 1.4866, suggesting that the adsorption of theophylline on mag-MIP-TRIM and DVB is favorable.

Dynamic adsorption of theophylline on magnetic MIPs

Adsorption kinetics is one of the most important characters which represent the adsorption efficiency. Figure 7 shows the dynamic curves for the adsorption of theophylline on mag-MIP-TRIM and mag-MIP-TRIM and DVB. Adsorption capacity increases rapidly at the beginning, and then adsorption rate decreases in later stage until reaching adsorption equilibrium. However, The mag-MIP-TRIM and DVB requires much shorter time to reach adsorption equilibrium than does the mag-MIP-TRIM. Two factors contribute to the faster adsorption equilibrium in the mag-MIP-TRIM and DVB. First, The mag-MIP-TRIM and DVB using TRIM/DVB (1 : 1, molar ratio) as cross-linker is more flexible than mag-MIP-TRIM using pure TRIM as cross-linker. The flexibility of mag-MIP-TRIM and DVB makes templates more accessible to the cavities of MIPs, and a state of adsorption equilibrium can be reached fast. Second, there are a large quantity of imprinted cavities and

"chemical pores" in mag-MIP-TRIM. Theophylline can permeate into the imprinted cavities through "chemical pores," and is adsorbed in imprinted cavities. The more adsorption in inner imprinted cavities is responsible for longer time to reach adsorption equilibrium on mag-MIP-TRIM.[17,18]

To discuss the mechanism of the adsorption process, the first-order equation was used to fit the experiment data. The first-order kinetic equation is expressed as

$$\ln(q_e - q) = \ln q_e - kt \qquad (7)$$

where q_e and q are the amount of theophylline adsorbed at equilibrium and at any time t, respectively. Linear plots of $\ln(q_e - q)$ versus t (Fig. 8) indicate the applicability of the above equation to the system studied. The value of q_e of mag-MIP-TRIM and mag-MIP-TRIM and DVB yielded by the intercept is 16.62 mg/g and 5.685 mg/g, respectively. The value of k calculated from the slope is 0.00336 min^{-1} for mag-MIP-TRIM and 0.0067 min^{-1} for mag-MIP-TRIM and DVB. The correlation coeficients (r^2) of mag-MIP-TRIM and mag-MIP-TRIM and DVB are higher than 0.99. The correlation coefficients are so near to 1, indicating that the dynamics of theophylline adsorption on both magnetic MIPs fit well with the first-order kinetic model.
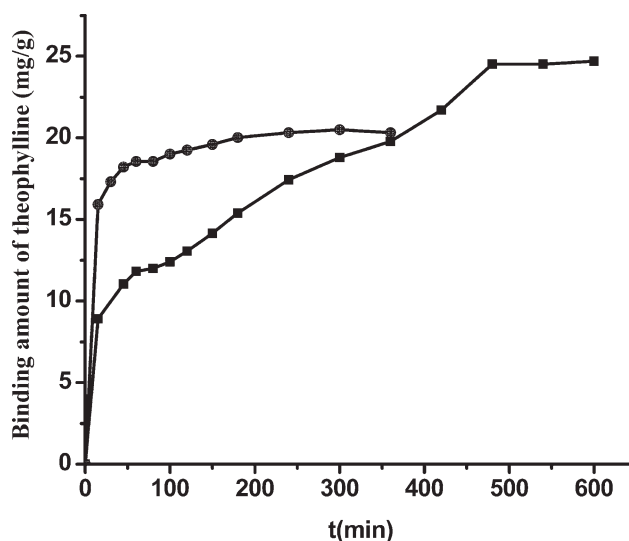

Figure 7 Dynamic curve for the adsorption of theophylline on mag-MIP-TRIM (■) and mag-MIP-TRIM and DVB (●).
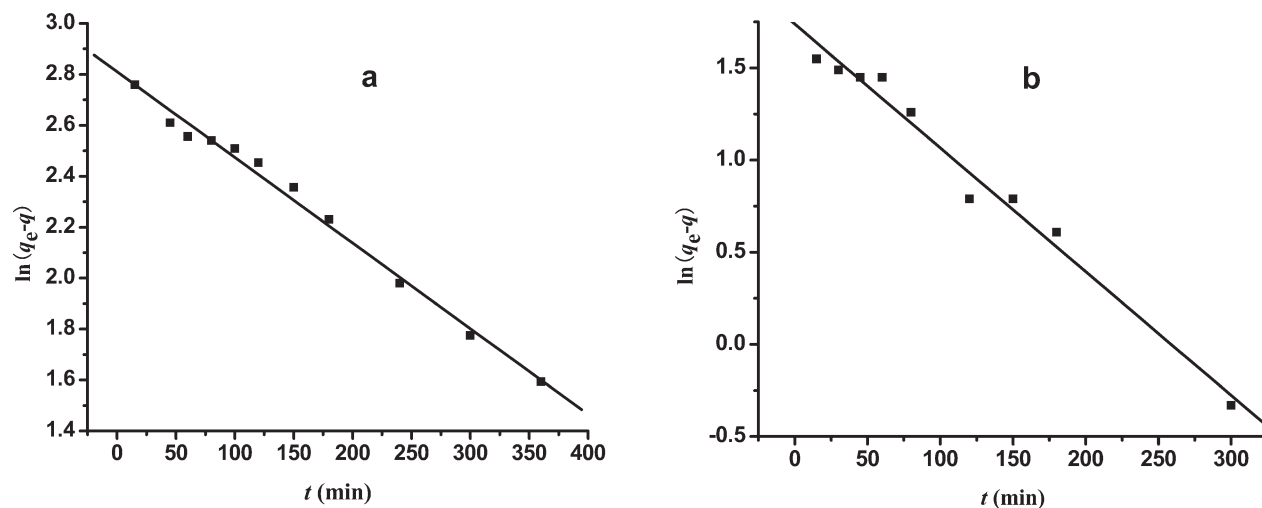
Figure 8 Relationship curve of $\ln(q_e - q)$ and time at 25°C.

CONCLUSIONS

A method based on "grafting from" method via suspension polymerization is developed to prepare magnetic MIPs in aqueous environment. The leakage of Fe_3O_4 nanoparticles from MIPs can be overcome in this study. The kinds of cross-linker have great effect on the adsorption capacity of magnetic MIPs. Both Mag-MIP-TRIM and DVB and mag-MIP-TRIM exhibit higher capacity for theophylline in aqueous environment than the corresponding magnetic NIPs, and Freundlich equation fits well for theophylline adsorption on both magnetic MIPs. In addition, the imprinting efficiency of mag-MIP-TRIM and DVB is much higher than that of mag-MIP-TRIM, meaning that the mixture of cross-linkers can improve the imprinting efficiency of magnetic MIPs. Both mag-MIP-TRIM and mag-MIP-TRIM and DVB exhibit good recognition properties for the template theophylline versus caffeine, and the selectivity of mag-MIP-TRIM toward theophylline is much higher than mag-MIP-TRIM and DVB. Dynamic adsorption of theophylline on magnetic MIPs shows that adsorption equilibrium on mag-MIP-TRIM and DVB reach faster than that on mag-MIP-TRIM, and the adsorption dynamics on both magnetic MIPs fit well with the first-order kinetic model.

References

1. Ou, J. J.; Li, X.; Feng, S.; Dong, J.; Dong, X. L.; Kong, L.; Ye, M. L.; Zou, H. F. Anal Chem 2007, 79, 639.
2. Mohamed, R.; Richoz-Payot, J.; Gremaud, E.; Mottier, P.; Yilmaz, E.; Tabet, J. C.; Guy, P. A. Anal Chem 2007, 79, 9557.
3. Urraca, J. L.; Moreno-Bondi, M. C.; Hall, A. J.; Sellergren, B. Anal Chem 2007, 79, 695.
4. Sun, H. W.; Qiao, F. X. J Chromatogr A 2008, 1212, 1.
5. Gros, M.; Pizzolato, T.; Petrovíc, M.; LópezdeAlda, M. J.; Barceló, D. J Chromatogr A 2008, 1189, 374.
6. Moullec, S. L.; Truong, L.; Montauban, C.; Begos, A.; Pichon, V.; Bellier, B. J Chromatogr A 2007, 1139, 171.
7. Yao, N.; Chen, H.; Lin, H.; Deng, C.; Zhang, X. J Chromatogr A 2008, 1185, 93.
8. Chen, L. G.; Liu, J.; Zeng, Q. L. J Chromatogr A 2009, 1216, 3710.
9. Li, Y.; Yin, X. F.; Chen, F. R.; Yang, H. H.; Zhuang, Z. X.; Wang, X. R. Macromolecules 2006, 39, 4497.
10. Tan, C. J.; Tong, Y. W. Anal Chem 2007, 79, 299.
11. Tan, C. J.; Chua, H. G.; Ker, K. H. Anal Chem 2008, 80, 683.
12. Pérez, N.; Whitcombe, M. J.; Vulfson, E. J Appl Polym Sci 2000, 77, 1851.
13. Wang, X.; Wang, L. Y.; He, X. W. Talanta 2009, 78, 327.
14. Ansell, R. J.; Mosbach, K. Analyst 1998, 123, 1611.
15. Chen, L. G.; Liu, J.; Zeng, Q. L. J Chromatogr A 2009, 1216, 3710.
16. Chen, L. G.; Zhang, X. P.; Sun, L.; Xu, Y.; Zeng, Q. L.; Wang, H.; Xu, H. Y.; Yu, A. M.; Zhang, H. Q.; Ding, L. J Agric Food Chem 2009, 57, 10073.
17. Lu, S. L.; Cheng, G. X.; Pang, X. S. J Appl Polym Sci 2009, 89, 3790.
18. Lu, S. L.; Cheng, G. X.; Pang, X. S. J Appl Polym Sci 2009, 99, 2401.
19. Zhang, Y.; Liu, R. J.; Hu, Y. L. Anal Chem 2009, 81, 967.
20. Hu, Y. L.; Liu, R. J.; Zhang, Y. Talanta 2009, 79, 576.
21. Timothy, V. W.; Timothy, E. P. J Am Chem Soc 2001, 123, 7497.
22. Timothy, V. W.; Timothy, E. P. J Am Chem Soc 1999, 121, 7409.
23. Sulitzky, C.; Ruckert, B.; Hall, A. J.; Lanza, F.; Unger, K.; Sellergren, B. Macromolecules 2002, 35, 79.
24. Quaglia, M.; De Lorenzi, E.; Sulitzky, C.; Caccialanza, G.; Sellergren, B. Electrophoresis 2003, 24, 952.
25. Schweitz, L. Anal Chem 2002, 74, 1192.
26. Wang, H. J.; Zhou, W. H.; Yin, X. F.; Zhuang, Z. X.; Yang, H. H.; Wang, X. R. J Am Chem Soc 2006, 128, 15954.
27. Bossi, A.; Piletsky, S. A.; Piletska, E. V.; Righetti, P. G.; Turner, A. P. F. Anal Chem 2001, 73, 5281.
28. Wang, X. B.; Ding, X. B.; Zheng, Z. H. Macromol Rapid Commun 2006, 27, 1180.
29. Piletska, E. V.; Guerreiro, A. R.; Romero-Guerra, M. Anal Chim Acta 2008, 607, 54.
30. Dirion, B.; Cobb, Z.; Schillinger, E.; Andersson, L. I.; Sellergren, B. J Am Chem Soc 2003, 125, 15101.
31. Gai, Q. Q.; Qu, F.; Liu, Z. J.; Dai, R. J.; Zhang, Y. K. J Chromatogr A 2010, 1217, 5035.
32. Umpleby, R. J.; Baxter, S. C.; Bode, M.; Berch, J. K.; Shah, R. N.; Shimizu, K. D. Anal Chim Acta 2001, 435, 35.
33. Kim, H.; Spivak, D. A. J Am Chem Soc 2003, 25, 11269.